Development of new methodologies to assess the structural integrity of the grouted joint of a 10-Megawatt wind turbine substructure*

Desarrollo de nuevas metodologías para evaluar la integridad estructural de una junta de monopilote de una subestructura de aerogenerador de 10 Megavatios**

Benjamín Santos Varela 1[a], Álvaro Rodríguez Ruiz[*,b] y David Fernández de Rucoba[c]

[a] Ingeniero industrial y mecánico. Centro tecnológico CTC. Responsable de mercado y desarrollo de negocio. [b] Ingeniero industrial. Centro tecnológico CTC. Técnico de Proyecto. [c] Dr. Ingeniero de caminos, canales y puertos. Centro tecnológico CTC. Técnico de Proyecto.

ABSTRACT

Fatigue and corrosion are two of the main degradation mechanisms in this type of support structures. The development of new models and methodologies for the analysis of these degradation mechanisms is crucial. Therefore, a methodology to analyse the behaviour of grouted joints has been developed considering the effect of corrosion on steel parts of the grouted joints. This methodology is applied to a case study based on data of a 10 MW offshore wind turbine.

RESUMEN

La fatiga y la corrosión son dos de los principales mecanismos de degradación en este tipo de subestructuras. El desarrollo de nuevos modelos y metodologías para el análisis de estos mecanismos de degradación es crucial. Por ello, se ha desarrollado una metodología para analizar el comportamiento de este tipo de juntas considerando el efecto de la corrosión en las partes de acero de las juntas de monopilote. Esta metodología se ha aplicado a un caso práctico basado en los datos de un aerogenerador marino de 10 MW.

KEYWORDS: grouted joint, fatigue, offshore wind turbine, corrosion, stiffness, shear keys.
PALABRAS CLAVE: Junta de monopilote, fatiga, aerogenerador marino, corrosión, rigidez, llaves de cortante.

1. Introduction

The connections between the transition piece and the monopile for wind turbine support structures are made by the means of grouted joints. Classically, the grouted joints for monopile substructures are built from the overlap of two cylindrical tubes: the transition piece and the pile**,** whose resulting annulus is filled with a high strength concrete. The grouted joints are efficient as they are easily constructible, and they allow to correct the possible misalignment of the pile due to driving errors. A typical construction process follows few steps: (1) the transition piece is jacked up at the pile top edge using temporary brackets; (2) the concrete is poured in the annulus and left for curing; and (3) after the concrete has hardened, the jack-ups are removed and the transition piece holds due to the passive friction resistance at the interfaces between the layers.

The passive friction resistance is achieved by means of two contributions. One is the chemical adhesive bond between the concrete and the steel, which has developed during the concreting process and the other is the

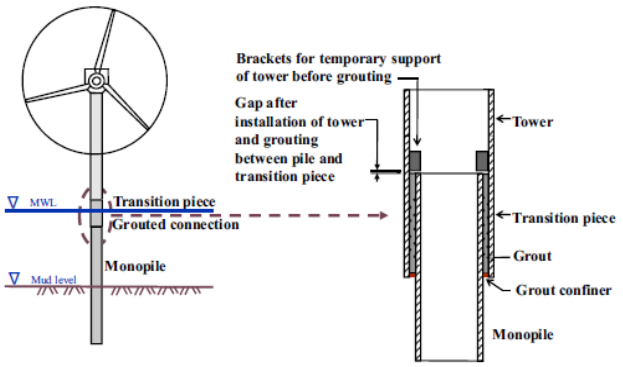

Figure 1. Scheme of cylindrical grouted connection in a monopile structure with the transition piece outside.

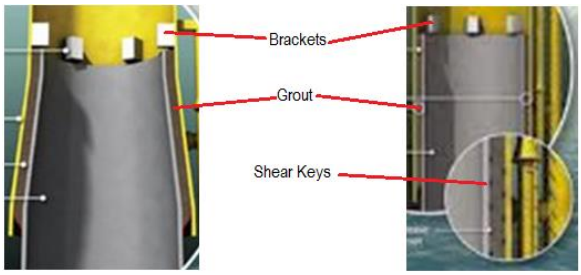

Figure 2. Conical grouted joint (left) vs. shear-keyed cylindrical grouted joint (right).

mechanical interlock between the rough concrete surface and the undulations at the steel surfaces. Moreover, during the loading operations the grout transfers the loads from the transition piece to the pile in the form of normal pressure and friction at the interfaces between the steel walls and the grout.

In order to ensure shear resistance, two solutions are proposed: conical grouted joint and shear-keyed grouted joints. A graphical example of each one is illustrated in Figure 2. The conical grouted joint is derived from the convention grouted joint by imposing a small conical angle (1° to 3°) to the overlapping tubes. With the conical angle, the structure weight effect on the connection decomposes into a shear component along the interfaces and a normal component to the interfaces. The latter component generates a permanent coulomb friction resistance, which prevents failure of the connection. The alternative solution contains shear keys on the inner faces of the cylindrical steel walls close to the connection middle in order to enhance the mechanical interlock. In either solution, as the passive mechanical interlock and the adhesive bond are not retained, therefore it is realistic to perform analysis without accounting for their respective contributions. Within IRPWIND project (funded by the European Union's 7th Programme for research, technological development and demonstration under grant agreement No. 609795) both types of geometry have been researched.

In the present paper only cylindrical grouted joints with shear keys, for a 10 MW wind turbine mounted on a monopile, will be studied. A new methodology to analyze the behavior of grouted joints considering the effect of fatigue and corrosion will be developed. This methodology and models are expected to increase our knowledge concerning the big issue of fatigue and corrosion in monopiles. Both are considered as the most important degradation mechanisms which increase the costs and compromise the reliability of these structures.

2. Reference turbine of 10 MW

The study is based on the 10 MW reference wind turbine developed by the Technical University of Denmark (DTU 10 MW RWT), consisting on a variable-speed, pitch-controlled and direct drive machine. Its key design parameters are presented in Table 1. The DTU 10 MW RWT has a rotor speed varying between 6.0 rpm and 9.6 rpm. It follows that the allowable support structure soft-soft natural frequency domain ranges within 0.00 Hz to 0.10 Hz, the soft-stiff domain ranges within 0.16 Hz to 0.30 Hz, and the stiff-stiff domain within 0.48 Hz and 0.60 Hz. In order to avoid resonance issues, an iterative procedure leads to a substructure with reference dimensions of 8500 mm outer diameter for the transition piece and 9000 mm outer diameter for the pile.

API RP2A WSD [1] recommends a min. thickness to account for driving induced stresses

t_{min} [mm] = 6.35 + D[mm] /100, which corresponds to about 96 mm. Survival to the limit states requires that the wall thickness of the pile ranges from 97 mm to 110 mm, and that of the transition piece is 80 mm thick. The penetration depth of the pile is configured to 30 m.

Table 1. Parameters of the DTU 10 MW wind turbine

Parameters	Values
Wind regime	5,7,9,…,21,23,25,50
Rotor type	3 bladed clockwise
Control	Variable speed
Cut-in, rated, cut-out wind speed	4,11.4,25 m/s
Rated power	10 MW
Rotor, hub diameter	178.3, 5.6 m
Hub height	119.0 m
Min., max. rotor speed	6.0, 9.6 rpm
Máx. Generator speed	480.0 rpm
Gearbox ratio	50
Máx. tip speed	90 m/s
Hub overhang	7.1 m
Shaft lift, coning angle	5.0º,-2.5º
Blade prebend	3.3 m
Rotor mass including hub	227962 kg
Nacelle mass	446036 kg
Tower mass	628442 kg

The environmental conditions used in this study have been adapted from Von Borstel [2]. The operational wind range is classified into 11 mean wind speed bins, each one linked to a particular sea state characterized by an expected significant wave height and a peak spectral period. The normal operational conditions have been modelled according to the IEC 61400-3 [3] design load case DLC 1.2. The wave height is modelled based on JONSWAP spectrum at the expected value of the sea state characteristics conditional on the mean wind speed. Misalignments of 0° or ±10° between the wind direction and the wave direction, yaw errors of 0° or ±10° between the wind direction and the rotor normal, and 6 seeds per mean

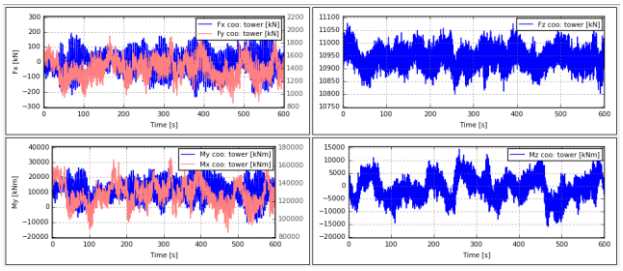

Figure 3. Scheme of cylindrical grouted connection in a monopile structure with the transition piece outside.

wind speed have been simulated for a total of 594 time series of 10-minute duration (600 seconds). The load assessment is carried out using the software package HAWC2 [4]. HAWC2 utilizes a multibody formulation, which joins different elastic bodies together using Timoshenko beam finite elements whereby their stiffness, mass, and damping are assembled into the governing equations of motion coupled to aerodynamic forces, whose aeroelastic solution is calculated using the Newmark-β method. The blade element momentum theory supplemented with Leishman Beddoes dynamic stall model and dynamic inflow is employed to represent the rotor unsteady aerodynamics.

The Mann turbulence model is used in load case simulations to represent the random Gaussian turbulent wind realizations blowing over the rotor. Random wave kinematics are computed according to the linear Airy model with Wheeler stretching. The hydrodynamic forces are calculated based on the Morison equation shown by Chakrabarti [5] with corrected coefficient of inertia to account for diffraction phenomenon shown by MacCamy [6]. Figure 3 illustrates a typical load time series (force and moment) generated from HAWC2 at the tower bottom at 11 m/s input mean wind speed.

3. Methodology

A cylindrical shear-keyed grouted connection with the transition piece placed outside the foundation pile has been studied and documented in this paper.

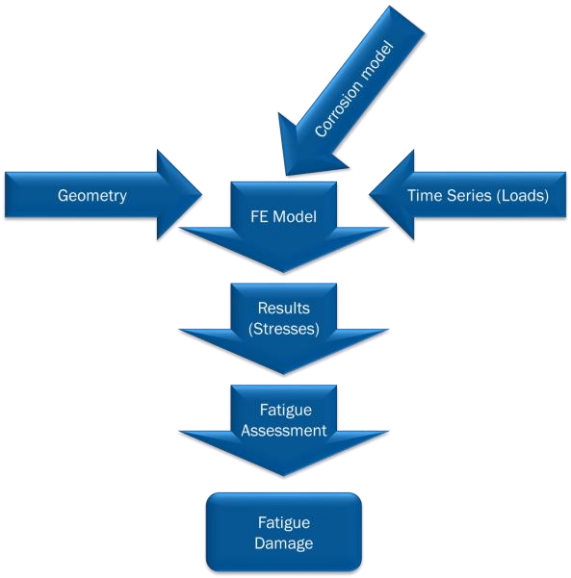

Figure 4. Methodology followed to assess damage due to fatigue.

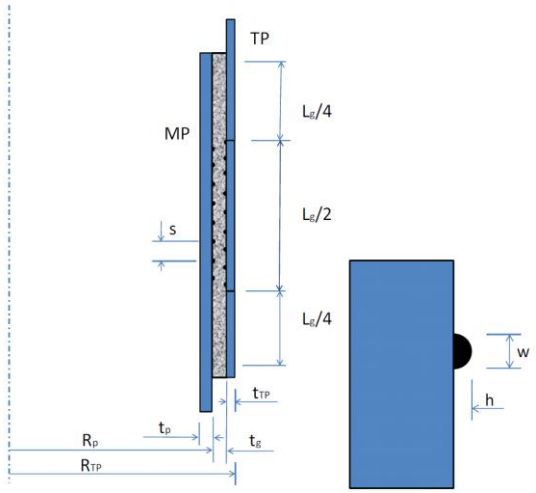

Figure 5. Symbols for grouted connections with shear keys.

Tubular (cylindrical) grouted connections in monopiles which are used to transfer axial force shall always be designed and constructed with shear keys. In general, the application of shear keys can improve the ultimate bearing capacity of a grouted connection significantly. The main issue of these types of connections is the fatigue, due to the stress concentrations around the shear keys, and corrosion because wind turbines operate in a very aggressive environment as described in DNVGL-ST-0126 [7]. For this reason, both degradation mechanisms will be evaluated simultaneously in the grouted joint. Fatigue is the most demanding loading condition; however, it is necessary to assess the maximum loads during storm conditions.

This paper describes the methodology followed to assess the fatigue damage of a cylindrical grouted connection with shear keys in a monopile that withstands a 10 MW offshore wind turbine. This methodology, illustrated in Figure 4, describes how the geometry of the cylindrical grouted connection, the corrosion model and the fatigue loads (time series) are the input of a parametric FE Model. This model runs all the fatigue time series for the given geometry and corrosion model and gives, as output, the stresses the model suffers. An assessment of these stresses is made for the design lifetime of the wind turbine, obtaining as final output the accumulated fatigue damage of the steel parts of the cylindrical grouted connection.

2.1 Geometry

The geometry of a cylindrical grouted shear-keyed connection is formed by two concentric tubular sections where the annulus is filled with grout. Figure 5 shows a scheme of a connection of this type with its main dimensions and symbols. Due to the geometrical restrictions to support the DTU 10 MW wind turbine, some parameters have fixed values and are listed as follows:

- Pile: diameter (D_{pile}), thickness (t_{pile}) and length (L_{pile}).
- Transition piece (TP): thickness (t_{TP}) and length (L_{TP}).

Additionally, two extra parameters have been defined to generate the different geometries for the evaluation with the parametric design methodology. First, the third dimension to totally define the geometry of the transition piece, its diameter (D_{TP}), which depends on the thickness of the grout (t_g) and the diameter of the pile

(D_{pile}). The second parameter is the vertical centre-to-centre distance between shear keys (s). Three different values have been assigned to these two parameters resulting, therefore, in nine combinations of geometry.

2.2 Time series

The life of a wind turbine can be represented by a set of design situations covering the most significant conditions that the wind turbine may experience. All relevant load cases with a reasonable probability of occurrence shall be considered, together with the behavior of the control and protection system. The design load cases (DLC) used to verify the structural integrity of a wind turbine shall be calculated by combining:

- Normal design situations and appropriate normal or extreme external conditions.
- Fault design situations and appropriate external conditions.
- Transportation, installation and maintenance design situations and appropriate external conditions.

The time series for the 10 MW wind turbine at the monopile is based on the aero-elastic model of the 10 MW DTU wind turbine. The time series are given at the interface between the transition piece and the tower.

2.2 Corrosion model

There are two main forms of corrosion that have big impact in offshore applications: general or uniform corrosion and pitting corrosion. The first directly influences structural strength. The second causes very localized and relatively severe penetration of the metal. As the second one is not predictable, only uniform corrosion is accounted. A corrosion rate for the whole operating life of the pile and transition piece has been considered. This corrosion rate is added as part of the effect of corrosion on the steel in the fatigue assessment. Recommended practice DNV-GL-RP-0416 [9] defines a corrosion rate of 0.3 mm/year for external surfaces and 0.1 mm/year for internal surfaces.

Table 2. Corrosion protection for pile and transition piece along the design life

Designed life (yrs.)	Pile	Transition Piece
0-5	Cathodic protection	Coating
5-10	Free corrosion	Coating
10-15	Free corrosion	Free corrosion
15-20	Free corrosion	Free corrosion

In the case described in this paper, it is considered that the transition piece only has its external surface in contact with seawater: Meanwhile, the pile has its internal surface in contact with seawater and part of the external surface which is not in contact with the grout. The protection used against corrosion in each part of the connection is indicated in Table 2.

The offshore wind turbine was designed for an operational lifetime of 20 years. It has been supposed that the cathodic protection in the pile works properly only the five first years, the rest of the life this part will suffer free corrosion. It means that from the fifth year on, the corrosion rate will be of 0.3 mm/year for external surfaces and 0.1 mm/year for internal surfaces. The transition piece has been assumed to be coated, working properly for 10 years. After that, free corrosion will take place in the external surface of the transition piece (0.3 mm/year). Corrosion affects the structural behavior of the pile and transition piece. Table 3 lists coefficients that increase the fatigue damage suffered by the components of the connection. This coefficient was obtained considering how the loss of section due to corrosion affects the moment of inertia of the two steel components of the connection. The coefficient for each service year is the relation between the initial moment of inertia and the moment of inertia the pile and the transition piece have this year, having into account that the moment of inertia will be decreased due to

corrosion plate thinning.

Table 3. Stress-rising coefficient in pile and transition piece

Service year	$K_{sr\ pile}$	$K_{sr\ TP}$
1-5	1.00000	1.00000
6	1.00220	1.00000
7	1.00441	1.00000
8	1.00663	1.00000
9	1.00886	1.00000
10	1.01110	1.00000
11	1.01335	1.00386
12	1.01561	1.00775
13	1.01787	1.01167
14	1.02015	1.01562
15	1.02243	1.01960
16	1.02473	1.02362
17	1.02704	1.02766
18	1.02935	1.03173
19	1.03168	1.03584
20	1.03401	1.03997

The highest rising in stresses is observed in the transition piece, around a value of 4% of increase in the last year of its designed life.

2.3 FE Model

A FE model of the cylindrical grouted joint has been developed and implemented in ANSYS FE program [8]. The model has been written in Ansys Parametric Design Language (APDL) in order to parametrize the geometry. The parameters of the geometry implemented in the FE model are grouped by zones as follows (rest of dimensions of the geometry depend on these):

- Pile: diameter (D_{pile}), thickness (t_{pile}) and length (L_{pile}).
- Transition piece: thickness (t_{TP}) and length (L_{TP}).
- Grout: thickness of the grout (t_{grout}).
- Shear keys: vertical centre-to-centre distance between shear keys (s), height (h) and width (w).

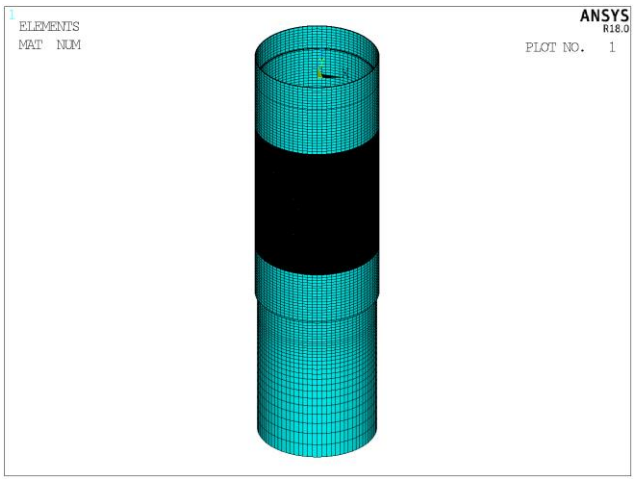

Figure 6. Mesh of the FE Model.

Once all values of the parameters have been defined, the code automatically generates the geometry and the mesh. 3-D solid elements (SOLID185) have been used in the pile, transition piece (TP) and grout and 3-D surfaced contacts (TARGE170 and CONTA174) have been set in the two interfaces: pile-grout and grout-TP.

The material properties used in the model are listed in Table 4.

Table 4. Material propeties in FE model.

Property	Grout	Steel of pile and TP	units
Young's Modulus	5.0 e+09	2.1e+11	Pa
Poisson's ratio	0.20	0.30	
Effective Density	2350	7850	kg/m^3

Figure 6 shows one of the 9 FE models created. The zone where the shear keys are placed has a higher mesh density (black area in Figure 6).

2.4 Fatigue assessment

In order to carry out the fatigue assessment of the steel parts of the connection, a methodology has been developed as illustrated in Figure 7. This methodology is respectively composed by 3 modules. These modules have been developed in

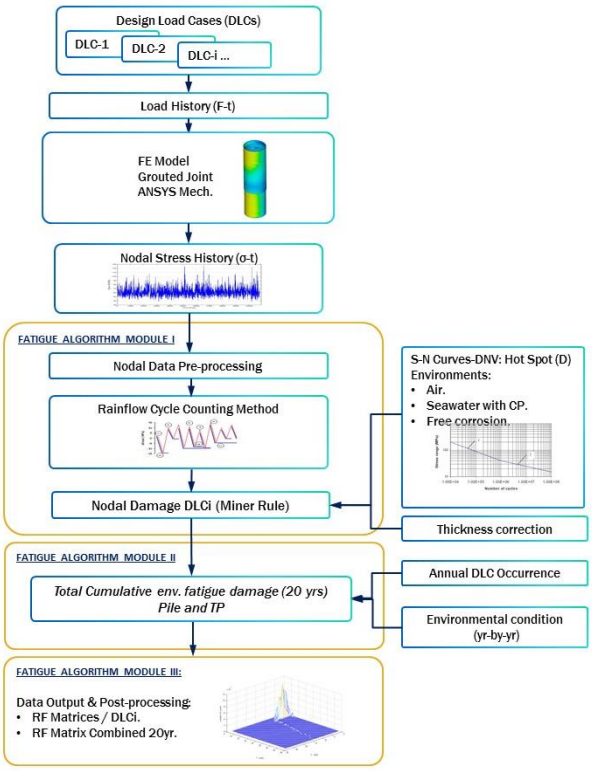

Figure 7. Fatigue assessment methodology flowchart.

MATLAB programming language and are explained in detail in the following lines.

In **Module I**, the first step is to pre-process the information considering nodal stresses. All the stress-time series for each DLC at the pile and transition piece (steel parts of the grouted joint) feed the module I of the methodology.

FE analyses of load-time series for 600 seconds of time frame were performed dynamically in the FE model for each DLC, as described previously using ANSYS.

As a first step, data of all nodes is pre-processed in module I, therefore, nodes from pile and transition piece are classified. According to the values often considered in normative as DNVGL-ST-0126 [7], a value of 20 years for service life is taken.

For each node and DLC, cycles are counted using Rainflow cycle counting method (ASTM E1049 [10]). Rainflow method is usually recommended for fatigue assessment and known as very accurate by authors like Lagoda, et alt. [11] and Yeter et alt. [12]. Rainflow algorithm provides values of number of cycles corresponding to the same stress range and mean stress.

In the next step, the number of cycles to failure is obtained by means of S-N Curves. Before calculating cycles to failure with the S-N Curves, stress range must be corrected with thickness according to DNVGL-RP-0005 [13]. This is due to S-N Curves were originally tested for a limited range of thickness. Each S-N curve correspond to a detail. In this case, Curve D recommended for hot spots is used. Three environmental conditions are evaluated for S-N Curve for all the studied nodes and DLCs: in air, in seawater with cathodic protection and free corrosion depending on the location of the nodes in the model.

In **Module II**, the previous results per DLC are collected and organized. Cumulated fatigue damage is estimated for the total service life of 20 years, considering the environmental effect in two ways: (1) from modified S-N curve with environment and, (2) in the corrosion plate thinning case by stress-rising. This effect is implemented in a year-by-year basis, including the selection of the S-N curve as summarized in Table 5, also based on the corrosion protection applied according to Table 5.

Table 5. S-N Curve selection related to corrosive environment (S-N Curve D)

Designed life (yrs.)	S-N Curve in Pile	S-N Curve in Transition Piece
0-5	In seawater with cathodic protection (CP)	In air
5-10	Free corrosion	In air
10-15	Free corrosion	Free corrosion
15-20	Free corrosion	Free corrosion

Palmgren-Miner Rule as shown by Palmgren [15] and Miner [16] is used to estimate the accumulated fatigue damage. Using this method, the formula is expressed as:

$$D_{DLC-node} = \sum \frac{n_i}{N_i} \quad (1)$$

Being n_i and N_i the number of cycles of each stress range and the number of cycles to failure according to the S-N Curve selected.

Table 6. S-N Curve D parameters (hot spot).

S-N Curve environment	$N \leq N_p$ cycles m1/loga1	$N \leq N_p$ cycles m2/loga2	N_p
In air	3.0/12.614	5.0/15.606	10^7
in seawater with CP	3.0/11.714	5.0/15.606	10^6
Free corrosion	3.0/11.687	-/-	-

The cumulative damage D is obtained with a modified version of the equation described in section 6.6.3 in DNVGL-ST-0126 [7]. This modified version is described for each node as follows:

$$D_{total-node} = \sum_{k=1}^{yr} \left(\sum_{j=1}^{m} f_{0,j} \cdot D_{DLC-node} \right) \quad (2)$$

Where $f_{0,j}$ is calculated as a quotient between time load and time series multiplied by the yearly occurrence of each DLC.

Finally, **Module III**, the last step in the methodology, analyzes and represents the results. Consequently, Rainflow matrices of each DLC are generated in module III for the most damaged node of both structural components, the pile and the transition piece. Furthermore, a combined matrix for the complete service-life (20 years) considering occurrence is defined and plotted for the nodes of the pile and transition piece.

5. Case study

Some parameters that define the geometry of the connection were fixed whose values are:

- Pile diameter (D_{pile}) = 9 m.
- Pile thickness (t_{pile}) = 97mm.
- Pile length (L_{pile}) = 56 m.
- Transition piece thickness (t_{TP}) = 80 mm.
- Transition piece length (L_{TP}) = 26 m.

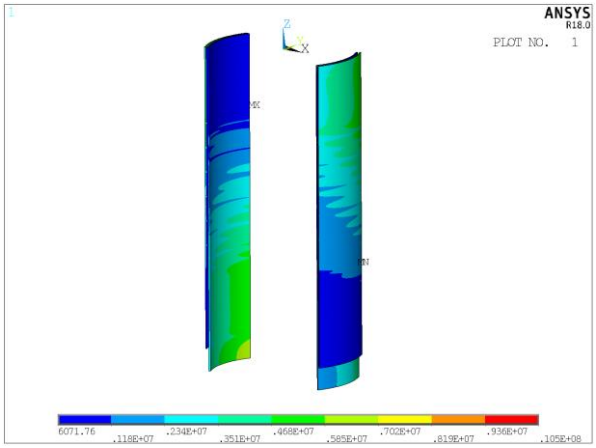

Figure 8. Example of stress distribution in most critical sections of the connection.

Once these parameters were fixed, three different values of s and three different values of t_{grout} were considered. Therefore, a total of nine geometries were studied (see Table 6).

Table 6. Geometries considered in case study depending on s and t_{grout}

Geom.	s (m)	t_{grout} (m)	h (m)	Shear keys in TP	Shear keys in pile
1	0.5	0.07	0.02	18	17
2		0.09			
3		0.11			
4	1.0	0.07	0.04	10	9
5		0.09			
6		0.11			
7	1.5	0.07	0.06	7	6
8		0.09			
9		0.11			

Considering all the parametric combinations, nine geometries were created in ANSYS. An ULS analysis was run for all of them to select the geometry that had the best structural behavior. This selected geometry was used to run the fatigue assessment. The loads applied to the geometries were the maximum values of the static load cases of the time series. Results of the static analysis concluded that geometry number 9 was the best option to run the fatigue analysis.

After selecting the most robust geometry,

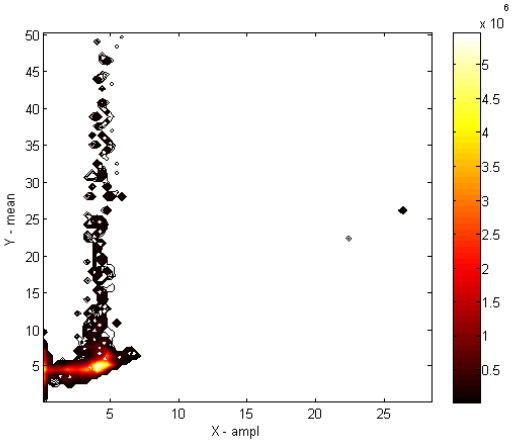

Figure 9. Rainflow combined matrix plot in pile.

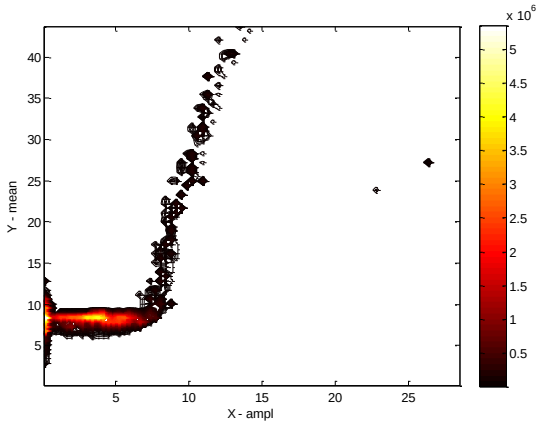

Figure 10. Rainflow combined matrix plot in TP.

the fatigue load case is described. It simulates the power production of an offshore wind turbine without faults performed for wind speeds in the entire operational range with normal turbulence. The cut in wind speed is 4 m/s and the cut-out wind speed is 25 m/s. There are time series for wind velocities from 5 m/s to 25 m/s (every 2 m/s). 3 wave seeds are used in 3 different directions. Yaw errors during normal operation are set to +/- 10°. Several seeds per wind speed and yaw error are used. The wind and wave directions have misaligned combinations for each wind speed. As 11 wind speeds are considered and there are 3 values of wind direction and 3 values of wave direction for each wind speed, there is a total of 99 time series. All the time series have a duration of 600 seconds. The results of the simulations were used for the fatigue assessment. Figure 8 shows a +/-30º portion of the most loaded part of the components of the connection.

In this case study, only environmental effects that affect S-N Curves were considered. Environmental effects are known to reduce significantly fatigue life of marine structures. Two categories of S-N Curves have been studied herein. S-N Curve D is firstly analyzed as is recommended for hot spot stresses according to DNVGL-RP-0005 [14]. This assessment covers the pile and transition piece separately.

Following the methodology described previously, different results for fatigue assessment were obtained depending on the component. Different results of damage were estimated for each component; while the pile is capable to withstand 20 years' service lifetime, transition piece surpasses the level of admissible damage (D > 1) in 20 nodes. These failed nodes are located at the upper shear key in the model. Values of maximum accumulated damage are shown below for the pile and the transition piece.

Table 7. Cumulative damage in pile and transition piece

Component	Max. Damage	Nº of failed nodes
Pile	0.8883	0
Transition piece	1.2060	20

It should be noted that the failed nodes are located in the edge that connect the shear key with the tube of the transition piece, where stresses are concentrated.

In the following graphs, plots of the combined Rainflow matrices are shown for the most fatigued node of the pile (see Figure 9) and of the transition piece (see Figure 10). In general, it is observed that transition piece node shows higher amplitudes compared to the counterpart in the pile.

6. Conclusions

A methodology to assess the influence of the

fatigue and corrosion in the structural integrity of the steel part of a grouted joint connection of a 10 MW wind turbine has been developed.

The effect of corrosion in fatigue due to plate thinning is necessary to be accounted, otherwise unconservative results are obtained.

A reduction of dynamic stresses is observed in the studied grouted joint between transition piece and pile as shown in the Rainflow matrices. Two main reasons have been identified: the first one is a higher moment of inertia of the tubular section for the pile compared to the transition piece, and the second one is the lower stiffness of the grout that may act as a damper for dynamic loads.

S-N Curve D the pile is safe, however a very small area of the transition piece exceeds fatigue life limit of 1. If S-N Curve C1 from DNVGL-RP-005 [14] was considered in both components, pile and transition piece would withstand to the experienced loads for 20 years lifetime (not included in this paper).

Acknowledgments

IRPWIND project (funded by the European Union's Seventh Programme for research, technological development and demonstration under grant agreement No. 609795).

References

[1] American Petroleum Institute, Recommended practice for planning, designing and constructing fixed offshore platforms — Working stress design. API RP 2A WSD, 2005.

[2] T. Von Borstel, INNWIND.EU Deliverable 4.3.1 – Design report – Reference Jacket, 2013.

[3] The International Electrotechnical Commission: Wind Turbines – Part 3: Design requirements for offshore wind turbines, IEC 61400-3 Ed 1, 2009.

[4] Larsen TJ, Hansen AM. How 2 HAWC2, the user's manual. DTU Risoe-R-1597, 2015.

[5] Chakrabarti S. Handbook of Offshore Engineering. Elsevier, 2005.

[6] MacCamy RC, Fuchs RA. Waves forces on piles: A diffraction theory. Corps of Engineers 1954; 1-17.

[7] DNV GL, Support structures for wind turbines, DNVGL-ST-0126, 2016.

[8] ANSYS Computer Program Release 18.0, ANSYS Inc, 2017.

[9] DNV GL, Recommended Practice DNV-GL-RP-0416, 1 Edition, 2016.

[10] MATLAB & Simulink version R2012a. Mathworks, 2012.

[11] ASTM E 1049-85 Standard Practices for Cycle Counting in Fatigue Analysis, 1996.

[12] Lagoda T., Macha, E., and Niesłony, A., Fatigue life calculation by means of the cycle counting and spectral methods under multiaxial random loading, Fatigue & Fracture Engineering Mater. Struct. 28, pp 409-420, 2004.

[13] Yeter B., Garbatov, Y., and Guedes Soares, C., Fatigue damage assessment of fixed offshore wind turbine tripod support structures, Engineering Structures, 101, 518-528, 2015.

[14] DNVGL, Recommended Practice DNV-GL-RP-0005, RP-C203: Fatigue design of offshore steel structures, 2014.

[15] Palmgren, A., Die Lebensdauer von Kugellagern, Zeitschrift des Vereins Deutscher Ingenieure, Vol. 68, pp. 339-341. 1924

[16] Miner, M.A., Cumulative damage in fatigue, Journal of Applied Mechanics, Vol. 12, pp.159-164, 1945.